Neutral Beam Divergence Due to Imperfect Magnetic Shielding

J.R. Conrad

November 1977

UWFDM-226

FUSION TECHNOLOGY INSTITUTE

UNIVERSITY OF WISCONSIN

MADISON WISCONSIN

Neutral Beam Divergence Due to Imperfect Magnetic Shielding

J.R. Conrad

Fusion Technology Institute
University of Wisconsin
1500 Engineering Drive
Madison, WI 53706

http://fti.neep.wisc.edu

November 1977

UWFDM-226

Neutral Beam Divergence Due To Imperfect Magnetic Shielding

J. R. Conrad

November 1977

UWFDM-226

Fusion Technology Program
Nuclear Engineering Department
University of Wisconsin
Madison, Wisconsin 53706

Abstract

The divergence of a neutral beam due to imperfect magnetic shielding of the gas cell neutralizer is considered. Coupled kinetic equations for the ion and neutral velocity distribution functions are solved. The deflection and divergence of the neutral beam are obtained from moments of the neutral distribution function.

I. Introduction

A fundamental requirement for neutral beam injectors used to heat and fuel fusion experiments is the ability to produce intense beams with low divergence. A lower limit on the attainable beam divergence is set by the ion temperature in the source used to generate the ion beam. Additional beam divergence is introduced by the single beamlet optics[1-3] of the ion accelerator and by imperfect steering of individual beamlets of multiaperture extractors.[4,5] One must also consider the effect of stray magnetic fields from the fusion experiment. Such fields may produce adverse effects on the ion source operation and are an additional source of beam divergence. The present paper treats the divergence of a neutral beam due to imperfect magnetic shielding of the gas cell neutralizer.

We will consider the idealized neutral beam injector shown schematically in Fig. 1. We assume that i) a monoenergetic,perfectly collimated beam of singly ionized (positive) atomic ions are extracted from the source and accelerated to velocity v_i in the x-direction, ii) individual beamlets from the source are focused on a common focal point so that the source, as viewed from the focal point, can be considered a point source, iii) the neutralizer cell is coupled directly to the ion source so that cold gas escaping from the source provides the charge exchange medium for neutralization, iv) infinite vacuum pumping is provided downstream of the neutralizer so that the beam composition beyond the neutralizer is unchanged in the drift space between the neutralizer and the target plasma, v) the cold gas efflux through the neutralizer is described by molecular flow so that the neutral density decreases linearly along the neutralizer, and finally vi) the transverse magnetic field B_0 in the y direction is uniform throughout the neutralizer of length L.

The physical origin of the stray magnetic field induced beam divergence and its qualitative dependence on beam energy can be described in advance of the detailed formulation and solution of the problem to follow. Consider an ion of mass m and charge +e with velocity v_i perpendicular to a uniform magnetic field B_o. Let ℓ_{cx} be the mean free path for charge exchange in the neutralizer cell. At very low energies (below a few keV), σ_{01}, the cross section for electron loss is very much smaller than σ_{10}, the cross section for electron capture. Thus at low energies, once the ion is neutralized it remains a neutral until it interacts with the target plasma (Fig. 2). For small deflections, the average perpendicular velocity will be $v_z = \ell_{cx}\,\Omega_i$ where $\Omega_i = q\,B_o/(mc)$ is the ion gyro frequency. At distances large compared to ℓ_{cx}, the average angular deflection will be $\overline{\Delta\theta} = \tan^{-1}(v_z/v_i) \approx \ell_{cx}\,\Omega_i/v_i$. In addition to this net average deflection, there will be a beam divergence due to the distribution of transverse velocities which in turn is due to the distribution of charge exchange path lengths. At intermediate and higher energies, σ_{01} becomes comparable to and exceeds σ_{10}. In this case the net average deflection and divergence will be larger, as a dynamic equilibrium develops between electron capture and loss (Fig. 2).

II. Beam Neutralization

Consider the neutralization of a monoenergetic, singly ionized positive atomic ion beam. The charge exchange neutralization process is described by

$$\frac{dF_o}{d\pi} = \sigma_{10}\,F_+ - \sigma_{01}\,F_o\,, \qquad (1)$$

$$\frac{dF_+}{d\pi} = \sigma_{01}\,F_o - \sigma_{10}\,F_+\,, \qquad (2)$$

where σ_{10} and σ_{01} are defined above, F_+ and F_o are respectively the ion and neutral fractions of the beam, and

$$\pi = \int_o^x n_n(x')dx' \tag{3}$$

is the thickness of the target neutral gas with density profile $n_n(x')$. For a close coupled neutralizer cell operating in the molecular flow regime[6], the neutral density will vary as

$$n_n(x) = n_o(1 - x/L) \tag{4}$$

where n_o is the neutral density at the source end of the neutralizer and where we have assumed that the neutral density at the downstream end of the neutralizer is very much less than n_o. We insert Eq. (4) into Eq. (3) to find

$$\pi(x) = n_o L \left[\left(\frac{x}{L}\right) - \frac{1}{2}\left(\frac{x}{L}\right)^2\right] . \tag{5}$$

If one solves Eqs. (1), (2) for the inital condition $F_+(\pi = 0) = 1$, subject to the constraint $F_o + F_+ = 1$ imposed by particle conservation, one obtains the well known result

$$F_o = F_o^\infty \{1 - \exp\left[-(\sigma_{01} + \sigma_{10})\pi\right]\} , \tag{6}$$

where

$$F_o^\infty \equiv \frac{\sigma_{10}}{\sigma_{10} + \sigma_{01}} \tag{7}$$

is the maximum possible neutralization fraction, i.e., the fraction which would be obtained in a neutralizer with infinite target thickness. The

final deflection and divergence of the neutral beam due to a transverse magnetic field in the neutralizer region will depend on F_0^∞. In Figure 3 we plot F_0^∞ versus beam energy for hydrogen, deuterium, and tritium using data from Ref. 7.

In a practical neutral beam system one is limited to a finite target thickness, so that F_0 at $x = L$ will be less than F_0^∞. In fact, vacuum pumping and space considerations may limit the maximum practical neutralization fraction to a value significantly less than F_0^∞. We will define ε to be the ratio of actual neutralization fraction to the maximum possible neutralization fraction, i.e.,

$$\varepsilon \equiv \frac{F_0\ (x = L)}{F_0^\infty} \ . \tag{8}$$

Clearly, if the neutral beam system is to be efficient, ε must be as close to unity as possible. From Eqs. (5)-(7), we then find that for a specified ε, the neutral density at the source end of the neutralizer must be given by

$$n_0 = - \frac{2\ell n(1-\varepsilon)}{(\sigma_{01}+\sigma_{10})L} \ , \tag{9}$$

so that finally the neutral profile is given by

$$n_n(x) = \begin{cases} \dfrac{\ell n(1-\varepsilon)^{-2}}{(\sigma_{01}+\sigma_{10})L}\left(1 - \dfrac{x}{L}\right) \text{ for } 0 \leq x \leq L \ , \\ 0 \text{ for } x < 0 \text{ and } x > L \ . \end{cases} \tag{10}$$

III. Kinetic Equations for Beam Divergence

We wish to determine the distribution of transverse velocities of neutrals exiting the neutralizer cell. The kinetic equations for the ion and neutral distribution functions f_i and f_o are

$$\frac{\partial f_i}{\partial t} + \vec{v} \cdot \vec{\nabla} f_i + \frac{e}{mc} (\vec{v} \times \vec{B}) \cdot \vec{\nabla}_v f_i = \nu_{01} f_o - \nu_{10} f_i , \tag{11}$$

$$\frac{\partial f_o}{\partial t} + \vec{v} \cdot \vec{\nabla} f_o = \nu_{10} f_i - \nu_{01} f_o . \tag{12}$$

where ν_{10} and ν_{01} are respectively the collision rates for electron capture and loss. If the ion beam is initially directed in the x-direction with velocity v_i and interacts with a transverse magnetic field in the y-direction, then with $\nu_{\alpha\beta} = n_n \sigma_{\alpha\beta} v_i$ the steady state kinetic equations are

$$\frac{\partial f_i}{\partial x} + \Omega_i \frac{\partial f_i}{\partial v_z} = n_n (\sigma_{01} f_o - \sigma_{10} f_i) , \tag{13}$$

$$\frac{\partial f_o}{\partial x} = n_n (\sigma_{10} f_i - \sigma_{01} f_o) . \tag{14}$$

In obtaining Eqs. (13) and (14) we have assumed that B is small enough that the velocity in the x-direction is unchanged to first order.
If we now insert Eq. (10) into Eqs. (13) and (14) and use the definition of F_o^∞ from Eq. (7) we find (for $0 \leq x \leq L$)

$$\frac{\partial f_i}{\partial x} + \Omega_i \frac{\partial f_i}{\partial v_z} = \frac{\ell n(1-\varepsilon)^{-2}}{L} \left(1 - \frac{x}{L}\right) \left[\left(1 - F_o^{\infty}\right) f_o - F_o^{\infty} f_i\right] , \quad (15)$$

$$\frac{\partial f_o}{\partial x} = \frac{\ell n(1-\varepsilon)^{-2}}{L} \left(1 - \frac{x}{L}\right) \left[F_o^{\infty} f_i - \left(1 - F_o^{\infty}\right) f_o\right] . \quad (16)$$

Finally, we introduce the dimensionless variables

$$\chi = \frac{x}{L} , \quad (17)$$

$$w = \frac{v_z}{\Omega_i L} , \quad (18)$$

and the definitions

$$c_1 = \left(1 - F_o^{\infty}\right) \ell n \left(1 - \varepsilon\right)^{-2} , \quad (19)$$

$$c_2 = F_o^{\infty} \ell n \left(1 - \varepsilon\right)^{-2} , \quad (20)$$

to obtain (for $0 \leq \chi \leq 1$)

$$\frac{\partial f_i}{\partial \chi} + \frac{\partial f_i}{\partial w} = (1 - \chi) \left[c_1 f_o - c_2 f_i\right] , \quad (21)$$

$$\frac{\partial f_o}{\partial \chi} = (1 - \chi) \left[c_2 f_i - c_i f_o\right] . \quad (22)$$

We assume that the initial beam incident on the neutralizer cell at $\chi = 0$ is fully ionized and perfectly collimated. The initial conditions are thus

$$f_o (0,w) = 0 , \quad (23)$$

$$f_i (0,w) = \delta(w) . \quad (24)$$

We now solve Eqns. (21) and (22) for $f_o(\chi,w)$. The beam deflection and divergence can then be obtained by examining $f_o(1,w)$, which is the distribution of transverse velocities of neutrals at the end of the neutralizer region. The coupled set of Eqs. (21) and (22) can be combined to yield a single, second order hyperbolic partial differential equation for $f_o(\chi,w)$. The general analytic solution of this equation is not tractable by elementary methods and we will resort to a numerical solution for the general case. However, it is possible to obtain an analytic solution for the limiting case $F_o^\infty \to 1$.

III. Analytic Solution for $F_o^\infty = 1$

For the limiting case $F_o^\infty = 1$, we have $c_1 = 0$ and $c_2 = \ln (1-\varepsilon)^{-2} \equiv C$, and thus Eqns. (21,22) become

$$\frac{\partial f_i}{\partial \chi} + \frac{\partial f_i}{\partial w} = - C(1-\chi) f_i \ , \tag{25}$$

$$\frac{\partial f_o}{\partial \chi} = C(1-\chi) f_i \ . \tag{26}$$

In this form it is possible to separate variables and obtain a solution using Fourier transforms. We define the Fourier transform pair

$$G(\chi,q) = \frac{1}{(2\pi)^{1/2}} \int_{-\infty}^{\infty} f_i(\chi,w)\, e^{\,iqw}\, dw \ , \tag{27}$$

$$f_i(\chi,w) = \frac{1}{(2\pi)^{1/2}} \int_{-\infty}^{\infty} G(\chi,q)\, e^{-iqw}\, dq \ . \tag{28}$$

We transform Eq. (25) to obtain

$$\frac{dG}{d\chi} + [-iq + C(1-\chi)]\, G = 0 \ , \tag{29}$$

which has the solution

$$G(\chi,q) = G(0,q)\ \exp[-(C - iq)\chi + \tfrac{1}{2} C\ \chi^2] \ . \qquad (30)$$

We transform the initial condition, Eq. (24) to obtain

$$G(0,q) = \frac{1}{(2\pi)^{1/2}} \ . \qquad (31)$$

The inverse transform obtained from Eq. (28), using Eqs. (30), (31) is then

$$f_i(\chi,w) = \delta(w-\chi)\ \exp[C(\tfrac{1}{2}\chi^2 - \chi)] \ \ (0 \leq \chi \leq 1) \ . \qquad (32)$$

Finally, we combine Eqs. (26) and (32) and integrate from $\chi = 0$ to $\chi = 1$, using the initial condition Eq. (23) to obtain the distribution of transverse velocities of neutrals exiting the cell. The result is

$$f_o(1,w) = \begin{cases} C\ (1-w)\ \exp[C\ (\tfrac{1}{2}w^2 - w)] \ , \ 0 \leq w \leq 1 \ , \\ 0 \text{ for } w < 0 \text{ and } w > 1 \ . \end{cases} \qquad (33)$$

We will compare this analytic solution for $F_o^\infty = 1$ with the numerical solution which will be obtained in the next section.

IV. Numerical Solution for the General Case

For the general case in which $F_o^\infty < 1$, we solve the coupled set Eqs. (21), (22) numerically using an explicit finite difference method. Grid points with spacing $\delta\chi$ and δw are constructed in the region $0 \leq \chi \leq 1$, and $0 \leq w \leq 1$. The values of $f_o(\chi,w)$ and $f_i(\chi,w)$ at the grid point (χ_j, w_k) are denoted by $f_o(j,k)$ and $f_i(j,k)$ where $\chi_j = j(\delta\chi)$ and $w_k = k(\delta w)$. The coupled set of Eqs. (20), (21) are differenced and solved according to

$$\frac{f_i(j,k+1) - f_i(j,k)}{\delta\chi} + \frac{f_i(j,k) - f_i(j-1,k)}{\delta w} = (1-\chi_j)[c_1 f_o(j-1,k) - c_2\ f_i(j-1,k)], \qquad (34)$$

$$\frac{f_o(j,k+1) - f_o(j,k)}{\delta\chi} = (1-\chi_j)\,[c_2\, f_i(j,k) - c_i\, f_o(j,k)] \,. \qquad (35)$$

In Fig. 4 we show solutions for the neutral velocity distribution at the exit end of the neutralizer, i.e. $f_o(1,w)$, for $\varepsilon = 0.95$ and a range of values of F_o^∞. These solutions were obtained with 100 grid points along the x-axis and 100 grid points along the w-axis. Also shown in Fig. 4 as a check on the numerical integration is a comparison with the analytic result, Eq. (33), for the special case $F_o^\infty = 1$.

As F_o^∞ decreases, fewer ions are neutralized and the total area under the curve $f_o(1,w)$ decreases accordingly. More important to the present discussion are the broadening and displacement of the distribution to higher transverse velocities which occur as F_o^∞ decreases. As F_o^∞ decreases, an ion entering the neutralizer remains ionized and is deflected by the magnetic field for a greater average total path length before being exiting as a neutral.

V. Neutral Beam Deflection and Divergence

The neutral beam mean deflection and divergence can now be obtained from the neutral beam distribution. The mean deflection $\langle\theta\rangle$ far from the neutralizer is given by $\langle\theta\rangle = \tan^{-1}(\langle v_z\rangle/v_i) \approx \langle v_z\rangle/v_i$ where $\langle v_z\rangle$ is the average neutral velocity in the z direction and we have assumed that $\langle v_z\rangle \ll v_i$. From Eq. (17) we have

$$\langle\theta\rangle = \frac{\Omega_i L \langle w\rangle}{v_i} \,, \qquad (36)$$

in which

$$\langle w\rangle \equiv \frac{1}{\varepsilon F_o^\infty} \int_0^1 w\, f_o(1,w)\, dw \,, \qquad (37)$$

and where we have made use of the normalization

$$\int_0^1 f_o(1,w)\, dw = \varepsilon F_o^\infty \,, \tag{38}$$

which can be obtained from Equations (21), (22).

Similarly we can obtain a measure of the neutral beam divergence $\langle\Delta\theta\rangle$ from

$$\langle\Delta\theta\rangle = \frac{\Omega_i L \langle(\Delta w)^2\rangle^{1/2}}{v_i} \,, \tag{39}$$

where

$$\langle(\Delta w)^2\rangle \equiv \langle w^2\rangle - \langle w\rangle^2 = \frac{1}{\varepsilon F_o^\infty} \int_0^1 w^2 f_o(1,w)\, dw - \langle w\rangle^2 \,. \tag{40}$$

While Eq. (40) provides a good measure of the beam divergence for cases where F_o^∞ is close to unity, it underestimates the divergence for small values of F_o^∞. The reason for this is that if F_o^∞ is small, $f_o(1,w)$ is very broad and velocity moments higher than second order become significant. Since the intrinsic beam profiles of most neutral beams is Gaussian in nature[1], we will define an "equivalent Gaussian divergence" half angle $(\Delta\theta)_g$ such that 85% of the neutrals lie between $\langle\theta\rangle - (\Delta\theta)_g$ and $\langle\theta\rangle + (\Delta\theta)_g$. This equivalent Gaussian half angle is given by

$$(\Delta\theta)_g = \frac{\Omega_i L\, (\Delta w)_g}{v_i} \,, \tag{41}$$

where we compute $(\Delta w)_g$ numerically from

$$\int_{\langle w\rangle - (\Delta w)_g}^{\langle w\rangle + (\Delta w)_g} f_o(1,w)\, dw = .85\, \varepsilon F_o^\infty \,, \tag{42}$$

using the normalization Eq. (38).

In Figs. 5-7 we plot the values of $\langle w \rangle$, $\langle (\Delta w)^2 \rangle^{1/2}$, and $(\Delta w)_g$ versus F_o^∞ for different values of ε. These values are obtained respectively from Eqs. (37), (40) and (42) using the numerical solutions of Eqs. (34), (35). Note that while $\langle (\Delta w)^2 \rangle^{1/2}$ and $(\Delta w)_g$ are comparable for F_o^∞ close to unity, $(\Delta w)_g$ is as much as 60% larger than $\langle (\Delta w)^2 \rangle^{1/2}$ for small X_o^∞. Consequently we will use only $(\Delta w)_g$ as a measure of the beam divergence.

VI. Discussion

In the design of neutral beam systems it is usually required that the maximum angular deflection $(\Delta\theta)_{max} = L\Omega_i/v_i$ be small in comparison with the intrinsic beam divergence or in comparison with the beam acceptance angle. The results of the present investigation (see Eq. (41) and Fig. 7) indicate that the above criterion for beam divergence is overly conservative by a factor ranging from three to six.

If one expresses B_o in gauss, L in centimeters and the neutral beam energy E_b in keV then one obtains from Eqs. (36) and (41) the mean angular displacement $\langle \theta \rangle$ and the "Gaussian equivalent" half angle divergence $(\Delta\theta)_g$

$$\left.\begin{array}{l} \langle \theta \rangle \text{ (degrees)} \\ (\Delta\theta)_g \text{ (degrees)} \end{array}\right\} = \frac{\left(\frac{m_p}{m}\right)^{1/2} B_o L}{79.8\,[E_b(\text{keV})]^{1/2}} \cdot \left\{\begin{array}{l} \langle w \rangle \\ (\Delta w)_g \,. \end{array}\right. \qquad (43)$$

where m_p is the proton mass and m is the mass of the beam ions. For typical values of L and E_b the mean angular displacement calculated from Eq. (43) is of order 0.02° to 0.1° per gauss of stray magnetic field B_o. For B_o as large as 10 G this simply requires a steering offset of 0.2° - 1.0°. Of greater importance is the beam divergence obtained from Eq. (43). In Table I we show

values of $(\Delta\theta)_g/B_o$ for several past, present and proposed neutral beam injector systems.[8-16] Also shown in this table are values of the stray magnetic field which have been measured or calculated in some of these systems.[8,9,12,15] It is necessary that the beam divergence due to the stray magnetic field be much less than the intrinsic field free divergence (typically one to two degrees) of the neutral beam system. In those systems for which residual magnetic fields have been reported,[8,9,12,15] this requirement is conservatively satisfied, especially in the design for the MX[12] injectors (see Table I).

Acknowledgements

This research was supported by the United States Department of Energy and the Wisconsin Electric Utility Research Foundation.

References

1. J.R. Coupland, T.S. Green, D.P. Hammond, and A.C. Riviere, Rev. Sci. Instrum. 44, 1258 (1973).
2. L.R. Grisham, C.C. Tsai, J.H. Whealton, and W.L. Stirling, Rev. Sci. Instrum. 48, 1037 (1977).
3. W.S. Cooper, K.H. Berkner, and R.V. Pyle, Nucl. Fusion 12, 263 (1972).
4. L.D. Stewart, J. Kim, and S. Matsuda, Rev. Sci. Instrum. 46, 1193 (1975).
5. T.S. Green and J.R. Coupland, Nucl. Instr. and Meth. 125, 197 (1975).
6. S. Dushman, Scientific Foundations of Vacuum Technique, John Wiley and Sons, Inc., New York, 1962, p. 87.
7. C.F. Barnett, J.A. Ray, E. Ricci, and M.I. Walker, Oak Ridge National Laboratory Report ORNL-5206, Vol. I, p. A.6.2.
8. A.K. Chargin and C.J. Anderson, "Solving Problems of Neutral Beam Injectors at LLL", Proc. of the Fifth Symp. on Engr. Problems of Fusion Research, Princeton University, 1973, IEEE Pub. No. 73CH0843-3-NPS, p. 421.
9. S.M. Hibbs, "Neutral Beam Injection in 2XIIB", Proc. of the Sixth Symp. on Engr. Problems of Fusion Research, San Diego, California, 1975, IEEE Pub. No. 75CH1097-5-NPS, p. 868.
10. T.H. Batzer, R.C. Burleigh, G.A. Carlson, W.L. Dexter, G.W. Hamilton, A.R. Harvey, R.G. Hickman, M.A. Hoffman, E.B. Hooper, R.W. Moir, R.L. Nielson, L.C. Pittenger, W.J. Silver, B.H. Smith, C.E. Taylor, R.W. Werner, and T.P. Wilcox, "Conceptual Design of a Mirror Reactor

for a Fusion Engineering Research Facility (FERF)", Lawrence Livermore Laboratory Report UCRL-51617 (Aug. 1974).

11. J.H. Fink, W.L. Barr, and G.W. Hamilton, Nucl. Fusion 15, 1067 (1975).

12. F.H. Coensgen, "MX Major Project Proposal", Lawrence Livermore Laboratory Report LLL-Prop-142.

13. R.S. Post, J. Kesner, J. Scharer, and R. Conn, Bull. Am. Phys. Soc. 22, 1094 (1977).

14. L.D. Stewart, R.C. Davis, J.C. Ezell, T.C. Jermigan, O.B. Morgan, W.L. Stirling, and R.E. Wright, "Design of High Power Injection Heaters for the Ormak System", Proc. of the Fifth Symp. on Engr. Problems of Fusion Research, Princeton University, 1973, IEEE Pub. No. 73CH0843-3-NPS, p. 406.

15. H.H. Haselton, W.K. Dagenhart, D.E. Schechter, L.D. Stewart, and W.L. Stirling, "PLT and Doublet III Neutral Beam Injection Systems", Proc. of the Sixth Symp. on Engr. Problems of Fusion Research, San Diego, California, 1975.

16. LBL/LLL CTR Staff, "TFTR Neutral Beam Injection System Conceptual Design", Lawrence Berkeley Laboratory Report LBL-3296.

TABLE I

DIVERGENCE DUE TO RESIDUAL MAGNETIC FIELDS IN EXISTING AND PROPOSED NEUTRAL BEAM SYSTEMS

EXPERIMENT	ION SPECIES	BEAM ENERGY E_b (keV)	NEUTRALIZER LENGTH L (cm)	BEAM DIVERGENCE PER GAUSS OF RESIDUAL FIELD[a] $(\Delta\theta)_g/B_o$ (deg./G)	MEASURED RESIDUAL MAGNETIC FIELD B_o (G)	BEAM DIVERGENCE $(\Delta\theta)_g$ (deg.)
2XII[8]	H	20	50	0.030	1	0.03
2XIIB[9]	D	20	80	0.032	3	0.09
FERF[10]	D	65	60	0.014	---	---
	T	100	60	0.011	---	---
MIRROR HYBRID REACTOR[11]	D	100	115	0.030	---	---
	T	150	115	0.020	---	---
MX[12]	D	20	25	0.010	0.5[b]	0.005
	D	80	50	0.013	0.5[b]	0.006
PHAEDRUS[13]	H	1.0-3.0	60	0.07-0.13	---	---
ORMAK[14]	H	26	80	0.045	---	---
PLT[15]	H	40	100	0.055	< few gauss	0.05-0.10
TFTR[16]	D	120	200	0.050	---	---

(a) assuming $\epsilon = 0.95$

(b) calculated

Figure Captions

Fig. 1. Schematic diagram of the idealized neutral beam injector, and the assumed cold neutral gas density profile in the neutralizer.

Fig. 2. Particle orbits through the neutralizer at high and low energy.

Fig. 3. Equilibrium fraction F_0^∞ of H^0, D^0 and T^0 in H_2, D_2 and T_2 respectively (data taken from Ref. 7).

Fig. 4. The distribution of transverse velocities of neutrals at the end of the neutralizer for different values of the equilibrium fraction.

Fig. 5. Average normalized transverse neutral velocity.

Fig. 6. Root mean square transverse neutral velocity.

Fig. 7. Equivalent Gaussian transverse neutral velocity width.

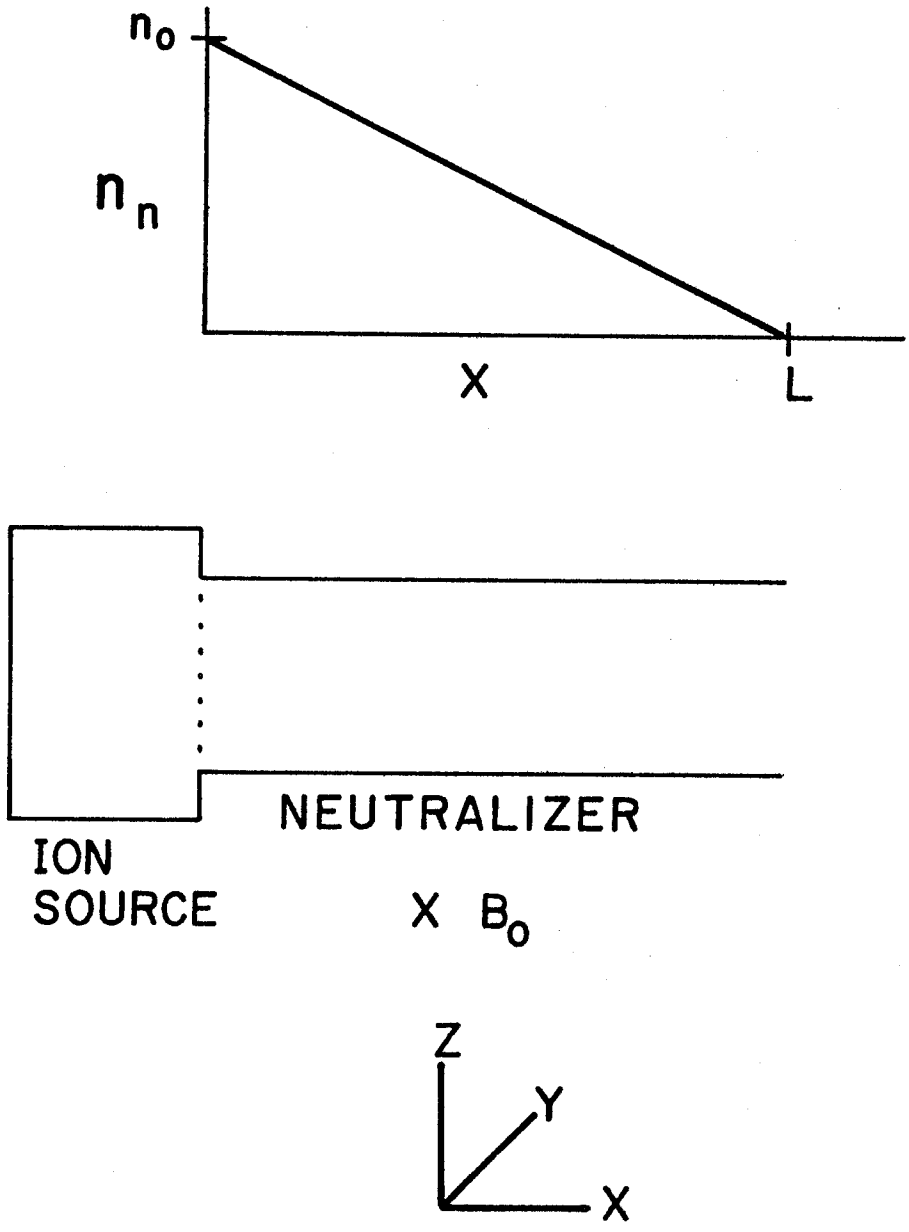

FIGURE 1

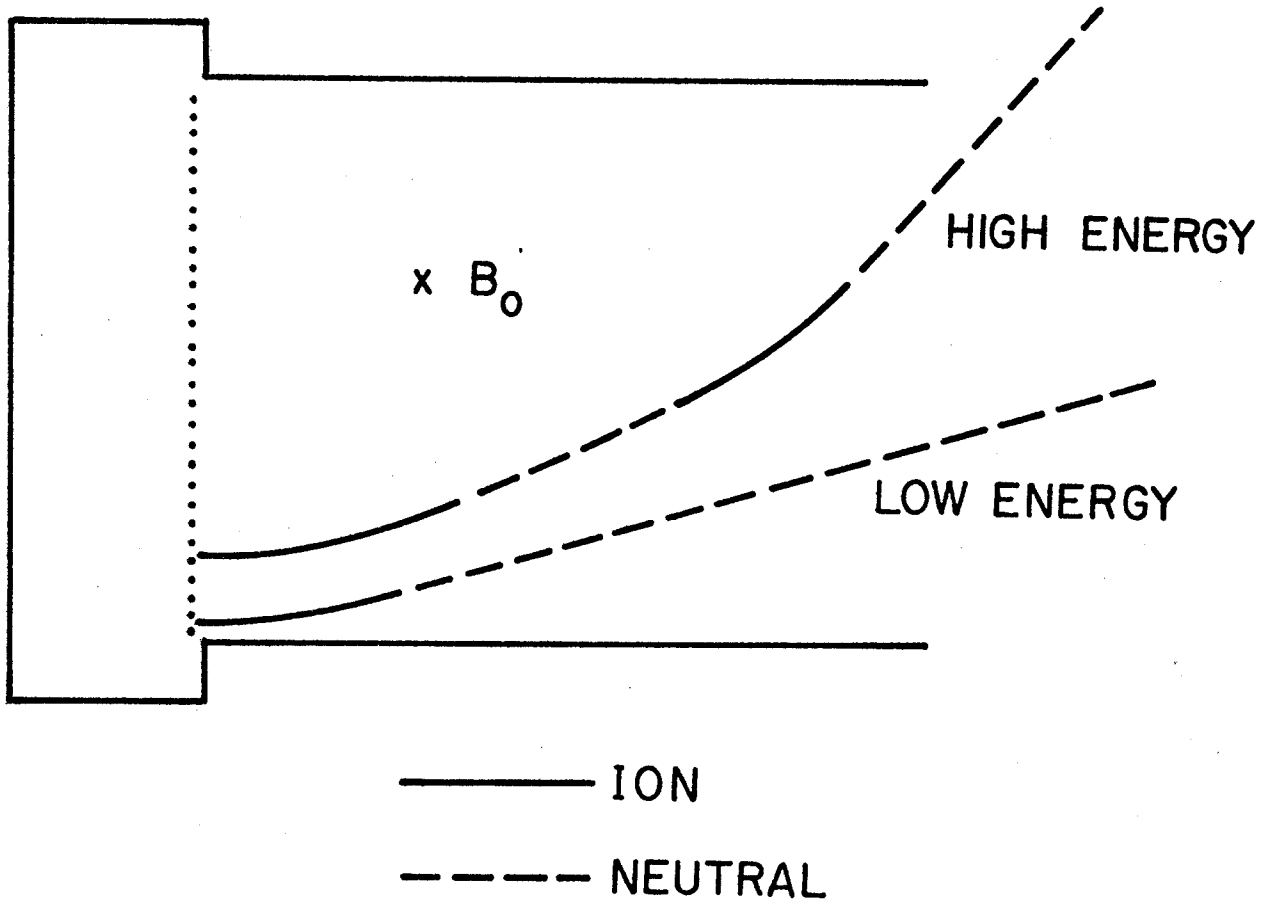

FIGURE 2

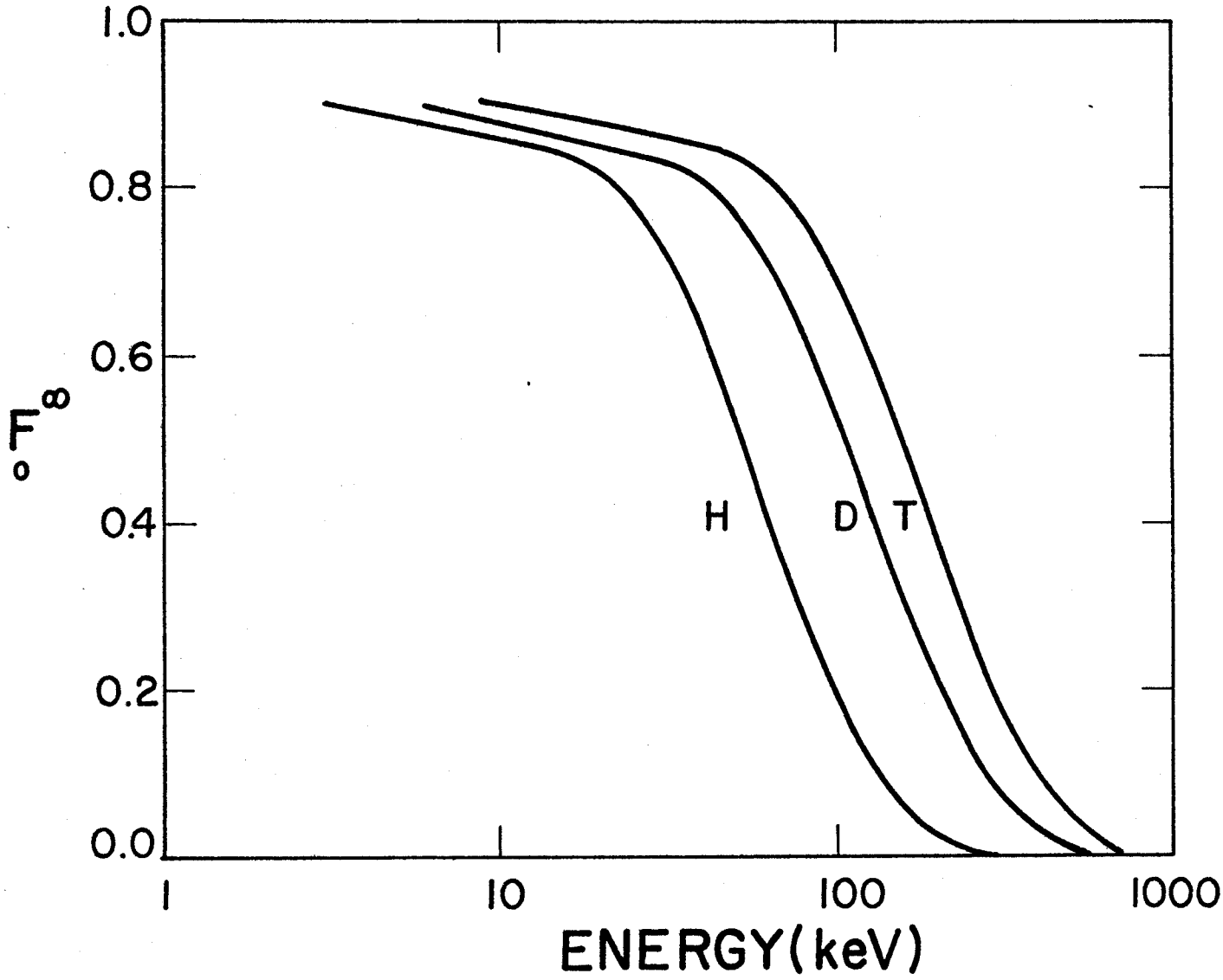

FIGURE 3

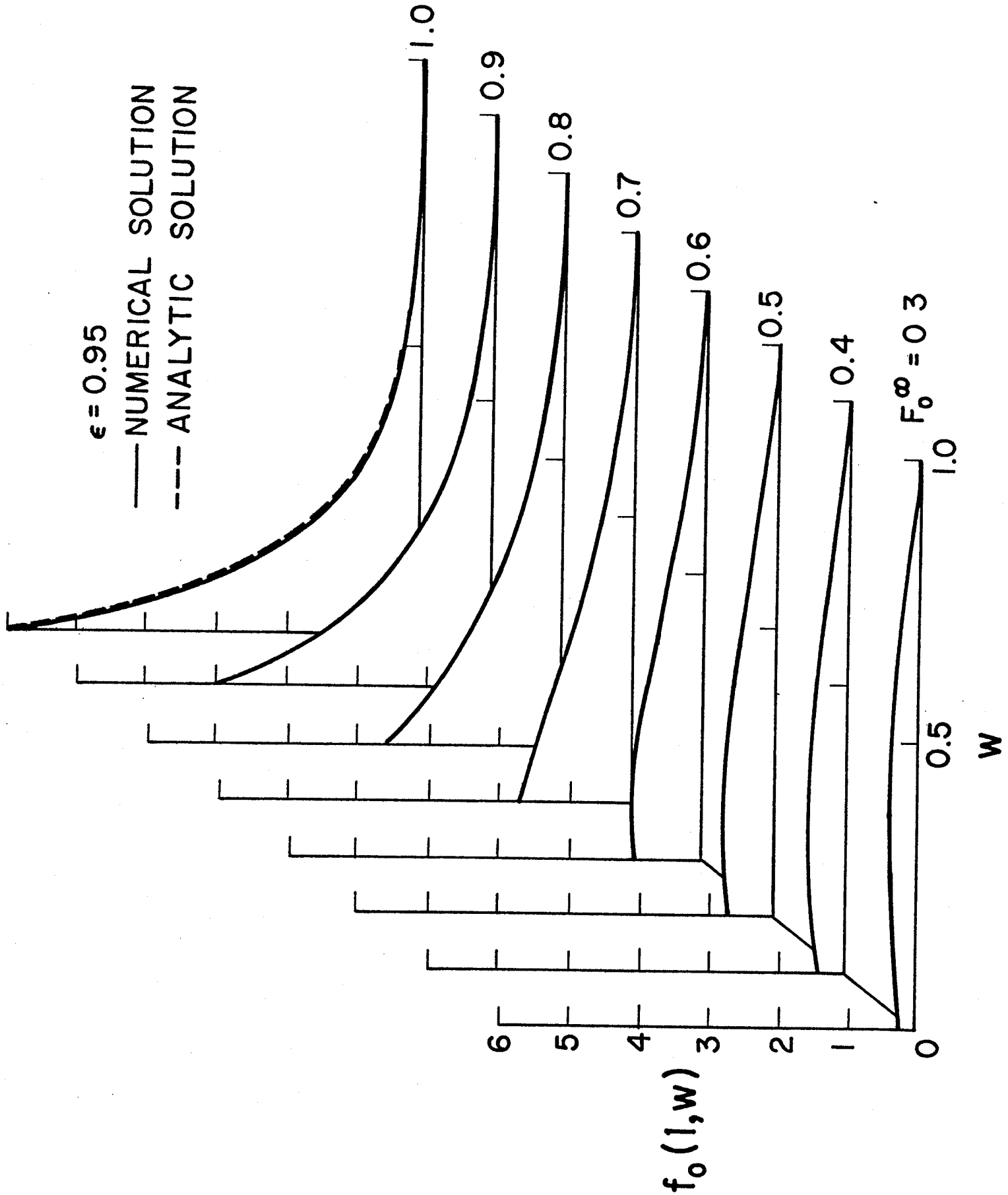
ε = 0.95
NUMERICAL SOLUTION
ANALYTIC SOLUTION
1.0
0.9
0.8
0.7
0.6
0.5
0.4
$F_0^\infty = 0.3$
1.0
0.5
W
$f_0(1,w)$
0
1
2
3
4
5
6

FIGURE 4

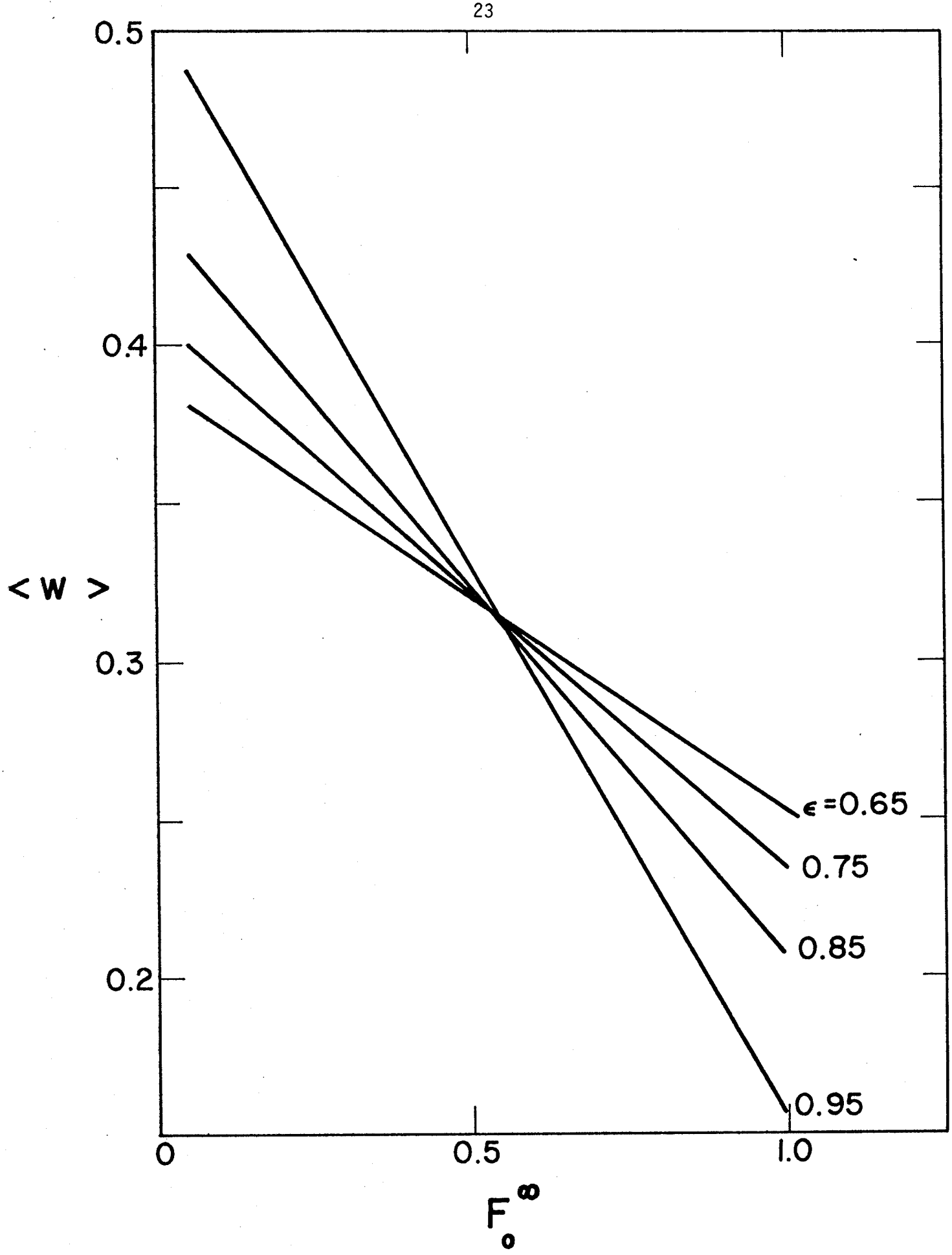

FIGURE 5

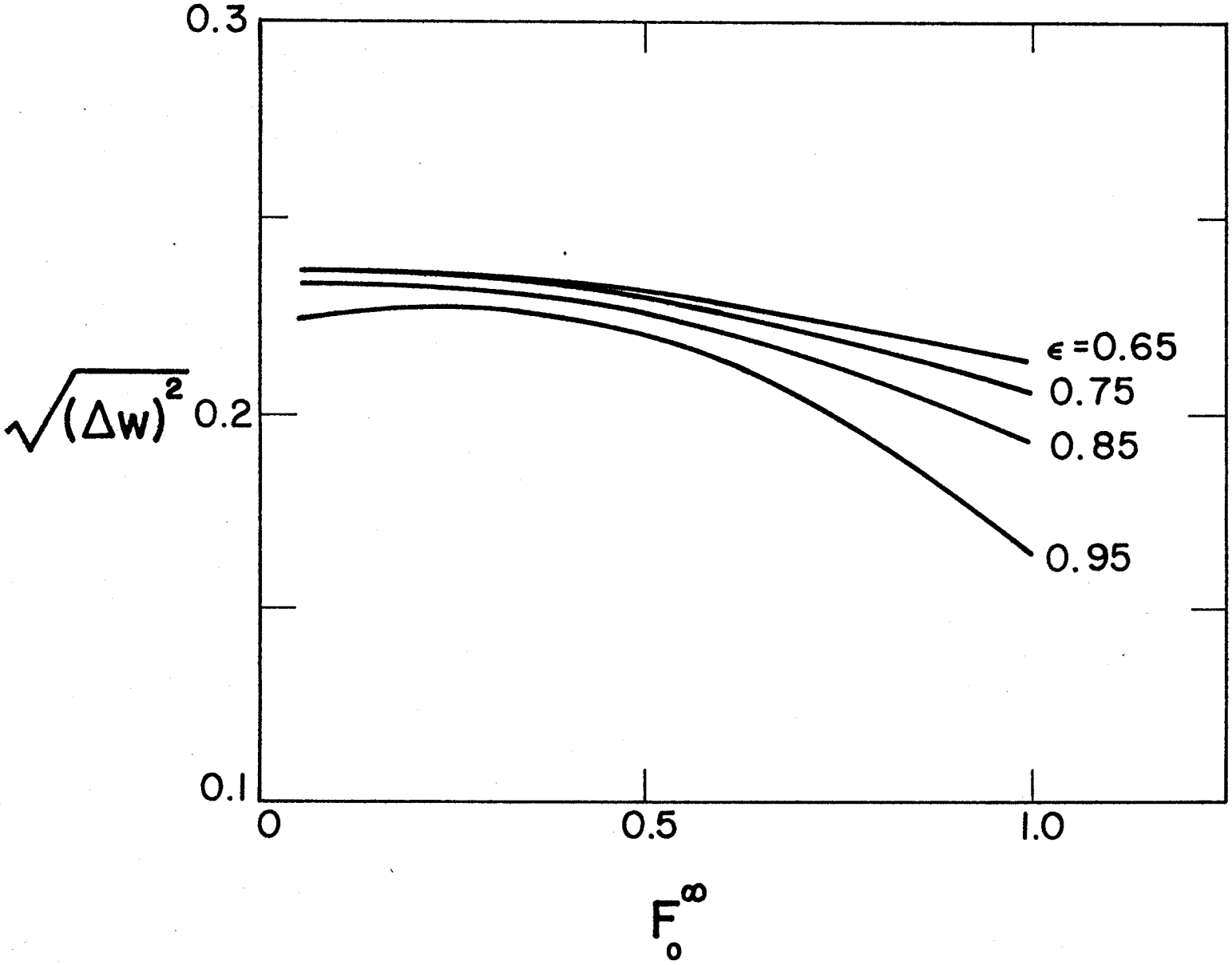

FIGURE 6

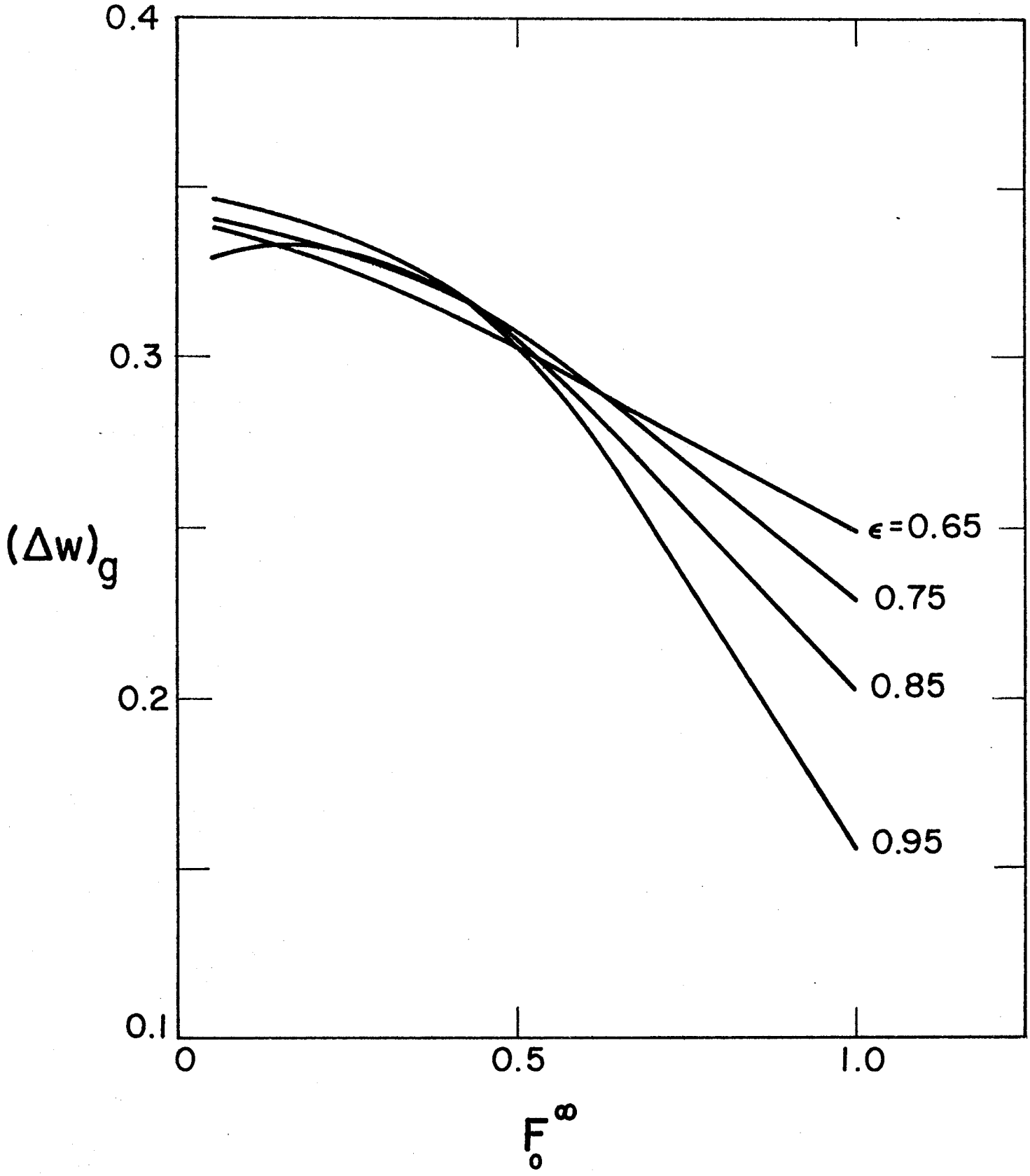

FIGURE 7